THE JOURNAL OF PHYSICAL CHEMISTRY LETTERS
A JOURNAL OF THE AMERICAN CHEMICAL SOCIETY

pubs.acs.org/JPCL

Letter

Pressure-Strengthened Carbon Fibers from Mesophase Pitch Carbonization Processes

Yanzhuo Wei, Jincong Chen, Haiyan Zhao,* and Xining Zang*

Cite This: J. Phys. Chem. Lett. 2022, 13, 3283−3289

Read Online

ACCESS | Metrics & More | Article Recommendations | Supporting Information

ABSTRACT: Little attention has been devoted to studying the pressures during the mesophase pitches carbonization processes and their effects on the as-produced carbon fibers' mechanical properties. Herein, we study the pressure-enhanced graphitization of mesophase pitch and the promoted tensile stresses of the produced carbon fibers using full atomistic simulations based on reactive force fields. Results show that pressures increase the tensile stress of as-produced fibers by 3.7−11 times under 1−6 GPa isotropic compressing pressure. The highest tensile stress can reach 4.39 GPa in carbonized coal tar pitch at 4000 K under 6 GPa. In experimental work, the pressurized laser-processed mesophase pitch generates less gas and shows more ordered carbonized structures in Raman spectra. This work provides a fundamental understanding of the reaction mechanism of carbon fiber production under pressure, and also illustrates a promising method to manufacture mesophase pitch-based carbon fibers with exceptional mechanical properties.

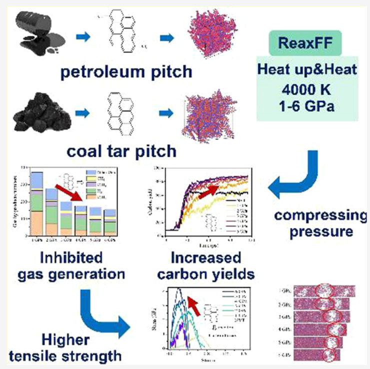

Carbon fiber (CF), one of the lightest and strongest materials, has long been applied in functional structures that require lightweight, including aerospace crafts, orthopedic implants, highspeed railways, etc. There are two typical types of CFs, i.e. polyacrylonitrile (PAN)-based CFs and pitch-based CFs. PAN-base CFs are synthesized by oxidation and polymerization of PAN precursors, followed by spinning and carbonization of the fibers.[1] Pitch-based fibers are produced following a similar procedure, while the low cost of coal-derived pitch precursors significantly decreased the price.[2] Mesophase pitches (MP) have aligned aromatic local structures, which result in better alignment of graphitic clusters in produced CFs, thus resulting in better mechanical strengths than CFs derived from isotropic pitches.[3] The high aromatic content and large local distance inherited from the precursors also result in high electrical conductivities and thermal conductivities, which are promising for applications for thermal management of electronics devices.[4]

Despite their low costs and high conductivities, mesophase pitch-based CFs, in general, have lower tensile strengths compared to PAN-based carbon fibers.[5] The improvement of mechanical strengths and the batch-to-batch consistencies of pitch-based CFs are critical for their large-scale manufacturing and versatile utilization. The current complex fabrication routines limit the fundamental study of reactions and properties, while the atomistic simulation could provide insights into the precursor-fabrication property by mimicking the high-temperature pyrolysis and alignment of aromatic sheets in various conditions. Furthermore, there are very few studies on how pressure could affect the carbonization and graphitization during the formation of CFs, yet in reality, the precursor molecules should have been pressurized in the spinning process and pyrolysis process.[6] On the carbon phase diagram, pressure is critical for sp^2 to sp^3 transition under extreme temperatures up to 3000 K.[7] The study of pressured carbonizations of MPs can reveal their evolution reaction pathways under pressure and can help to optimize the screening of MP precursors and processing parameters for CFs with higher modulus and tensile strength.

In this work, we employ molecular dynamics simulations using a reactive force field (Reaxff) to investigate the structural and chemical evolution of two typical MPs, i.e. petroleum-derived pitch and coal tar-derived pitch, at high temperature and specifically under high pressure from 1 to 6 GPa. In the MD simulation, two kinds of MP precursors are randomly put in boxes to generate configurations with a density of 1.5 g/cm^3. After the equilibration, structures are heated up to 4000 K and heated with pressure from 1 to 6 GPa to simulate the MPs pyrolysis reaction and carbonized structures are tested by using Airebo-MD for tensile strengths. The computational details are provided in the Supporting Information (Figure S1). To verify the effect of pressure in carbonization of MP, the pressure condition is introduced in the laser processing of MP as an experimental part. Our results provide a molecular-scale understanding of the mechanism of pressurized carbon fiber

Received: March 6, 2022
Accepted: April 4, 2022

https://doi.org/10.1021/acs.jpclett.2c00664
J. Phys. Chem. Lett. 2022, 13, 3283−3289

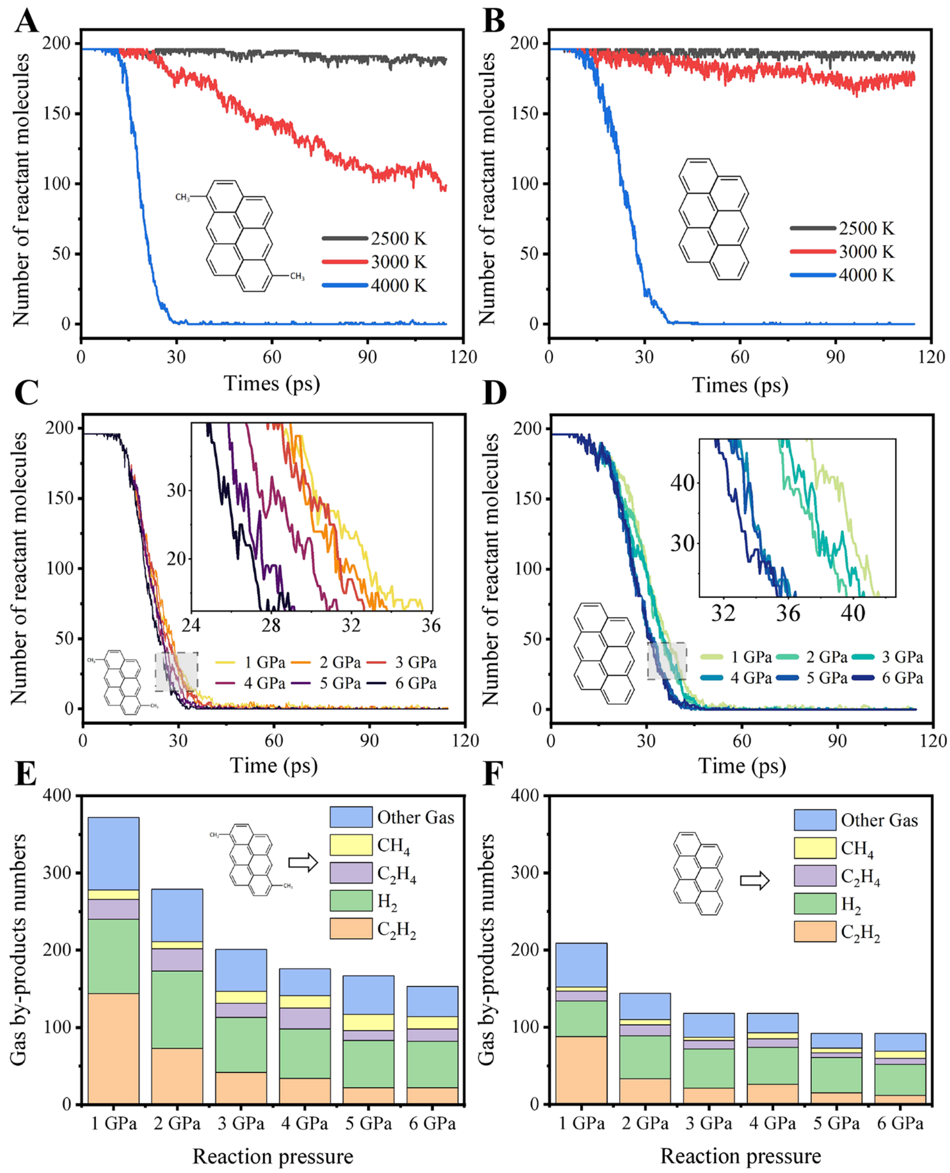

Figure 1. (A) Petroleum-derived Pitch (PP, $C_{24}H_{16}$) molecule consumption rates heated up to different temperatures in confined volume and NVT ensemble. (B) Coal Tar-derived Pitch (CTP, $C_{22}H_{12}$) molecule consumption rates heated up to different temperatures in confined volume and NVT ensemble. Two kinds of reactants are mostly consumed at 30 and 33 ps at 4000 K. (C) PP ($C_{24}H_{16}$) molecule consumption rates heated up to 4000 K under different pressures from 1 to 6 GPa. (D) CTP ($C_{22}H_{12}$) molecule consumption rates heated up to 4000 K under different pressures from 1 to 6 GPa. (E) Light (gas) byproduct decomposed from PP ($C_{24}H_{16}$). (F) Gas byproduct decomposed from CTP ($C_{22}H_{12}$).

production, which may enable carbon fibers with exceptional mechanical properties by adjusting the processing method of mesophase pitch.

Precursor Consumption and Gaseous Byproducts. Three temperatures at 2500, 3000, and 4000 K are tested by heating the relaxed MP structures using NVT ensemble.[8] As shown in Figure 1A and 1B, Petroleum-derived Pitch (PP) and Coal Tar-derived Pitch (CTP) molecules' consumption rates increase with the rise of temperature due to increased reaction rates at high temperatures, and the CTP system shows a lower consumption rate at the same temperature compared to that of PP. Considering the only difference between CTP and PP molecules is the presence of two more methyl groups, the above results indicate that methyl groups can promote the reaction activity of pitches. Besides, precursors heated in the NVT ensemble at 4000 K are set as control groups. Figure 1C and 1D show that the effect of increasing pressures on the consumption rates of reactant molecules is not as significant as that of temperature, especially under 1, 2, and 3 GPa, where the consumption curves of the reactants almost overlap. Above 4 GPa, the reaction rates begin to increase with the increase of the pressures in both cases of PP and CTP.

In the processes of reactant consumptions, the distribution of four major kinds of gas byproducts (CH_4, C_2H_4, H_2, C_2H_2) and the other gas byproducts are generated by the end of simulations. These four gas byproducts added up to more than 85% of the total gas molecules, wherein H_2 shows the highest amount. With the increase of pressure, the gas decreases by 56.0% and 58.9% in CTP and PP, respectively. C_2H_2 decreases by 86.4% and 84.7% in the heating process of CTP and PP; H_2 decreases by 13.0% and 37.5% in the heating process of CTP and PP. Such results indicate that the most significant suppression of degassing occurs in unsaturated gas such as C_2H_2. The major outgas hydrogen is consistent with most

https://doi.org/10.1021/acs.jpclett.2c00664
J. Phys. Chem. Lett. 2022, 13, 3283−3289

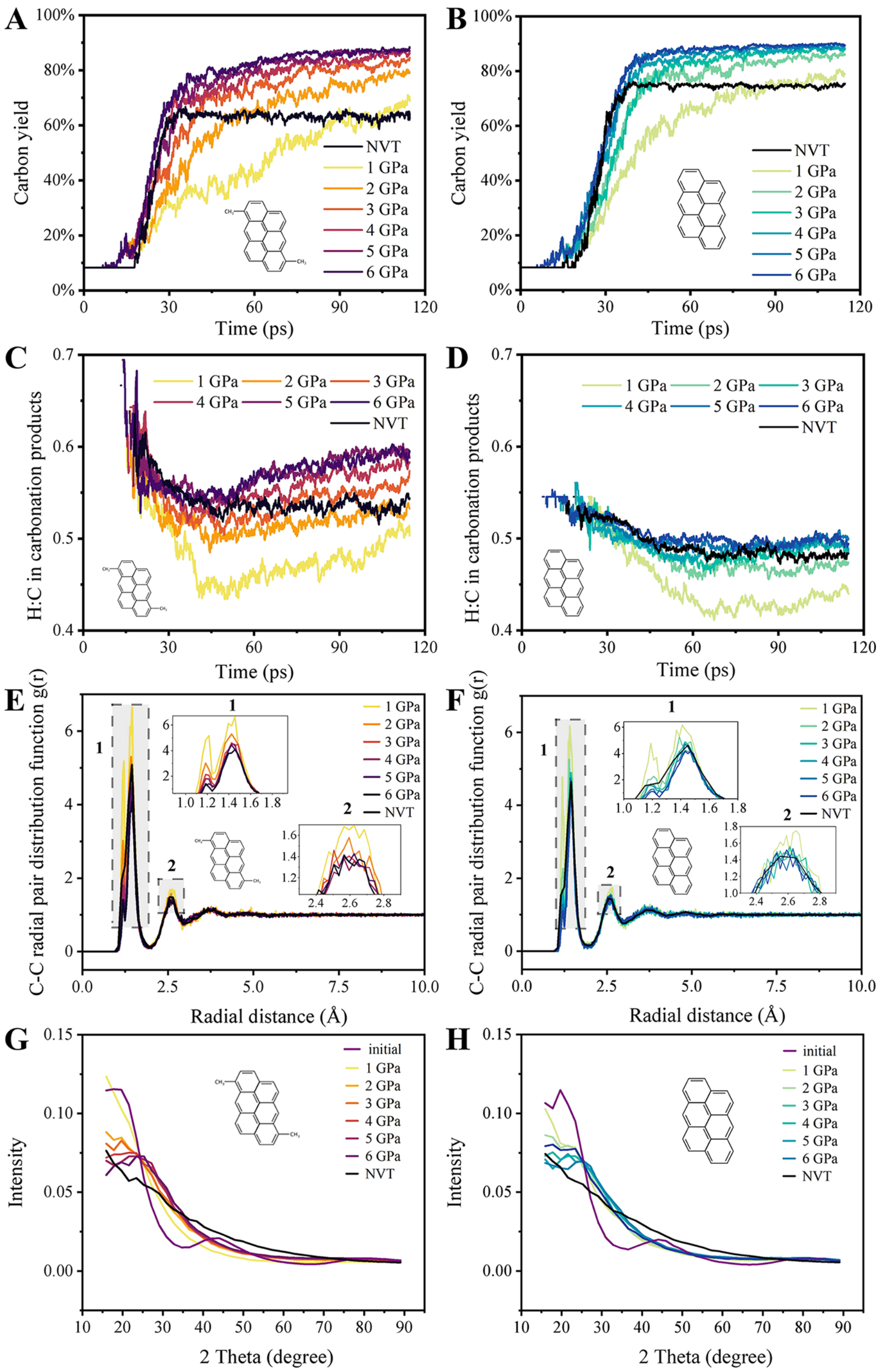

Figure 2. (A) CF yield as a function of time from 196 PP ($C_{24}H_{16}$) molecules. (B) CF yield from 196 CTP ($C_{22}H_{12}$). (C) H:C ratios of CFs as a function of time from 196 PP ($C_{24}H_{16}$) molecules. (D) H:C ratios of CFs from 196 CTP ($C_{22}H_{12}$) molecules. (E) C−C radial pair distribution functions (RDF) of CFs from 196 PP($C_{24}H_{16}$) molecules. (F) C−C RDF of CFs from 196 CTP($C_{22}H_{12}$) molecules. (G) XRD spectra of the initial system and CFs from 196 PP($C_{24}H_{16}$) molecules. (H) XRD spectra of the initial system and CFs from 196 CTP($C_{22}H_{12}$) molecules. Curve "NVT" corresponds to precursors in NVT ensemble as a control group (without fixed pressure).

experimental results of petroleum dehydrogenation reactions upon heating.[9] Meanwhile, the gaseous byproducts by CTP precursors are 33%−48% less than PP, and the variety of gas products by CTP is 2−4 less than that of PP precursors, which reflects fewer pathways for PP's decomposition.[8]

Carbonization and Graphitization. Figure 2A and 2B show the change of carbon yield over time, where the carbon yield is defined as the proportion of the carbon numbers in solid products out of carbon numbers in the whole system. The criterion to screen solid products is whether the total number of carbon atoms in the molecule exceeds 40.[9] With the increase of pressure, the completion time of Stage I (carbon yield increases rapidly) is reduced by 44.8% in PP and 13% in CTP (from 2 to 6 GPa), while the carbon yield of the whole process is improved from 73% to 96.1% in PP and from 84% to 98.1% in CTP. Compared to the control group, the results indicate that the pressure both accelerates the carbonization process and helps contain a high carbonization yield. Experimental work proposed similar improvement of carbonization yield under pressure.[10] Under the same pressure condition, PP

https://doi.org/10.1021/acs.jpclett.2c00664
J. Phys. Chem. Lett. 2022, 13, 3283−3289

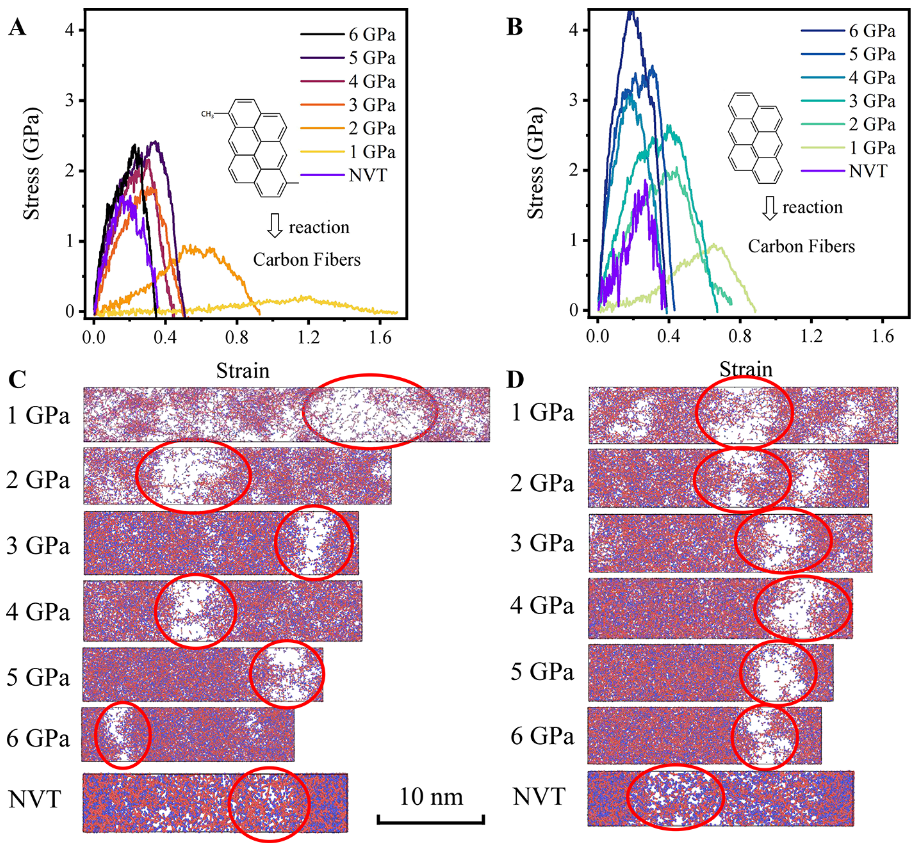

Figure 3. (A) Stress−strain curve of CF from 196 PP ($C_{24}H_{16}$) molecules. (B) Stress−strain curve of CF from 196 CTP ($C_{22}H_{12}$) molecules. (C) Visualization of tensile fractures in CF from 196 PP($C_{24}H_{16}$) molecules. (D) Visualization of tensile fractures in CF from 196 CTP ($C_{22}H_{12}$) molecules. Curve "NVT" corresponds to precursors in NVT ensemble as a control group (without fixed pressure).

precursors complete the carbonization stage I in a shorter time and the carbonization rate at the end of stage I is lower than that of the CTP precursor. These results can be attributed to more decomposition pathways of PP precursors with more secondary decomposition reactions occurring in the carbonization process, which interfere with the major carbonization reactions. The carbonization ratio of the final reaction is between 65% and 90%, similar to the description of pitch-based carbon fibers in experimental research.[11]

As shown in Figure 2C and 2D, the significant decreases in H:C ratios in PP (24.6%) and CTP (12.2%) molecules in stage I correspond to their rapid dehydrogenation and carbonization, which slow down when the major carbon solid frames form. The slight rise of the H:C ratio in PP (by 6%) and CTP (by 1.67%) upon longer heating time can be attributed to the recombination of gas molecules, majorly hydrogen and hydrocarbons, with the solid carbon under extreme pressure. With long enough simulation time, we estimate that the final H:C ratio will converge around 0.67 in PP and 0.54 in CTP, respectively. The depression of gas molecules during the mesophase pitch pyrolysis has also been observed in the experimental work,[12] suggesting that the evolution of hydrocarbon gases from the precursors is depressed.

Figure 2E and 2F show the C−C radial distribution function of CF produced by PP and CTP at the end of the simulation. The first peak around 1.21 Å in the figure corresponds to the length of the C−C triple bond after *sp* hybridization, reflecting the proportion of the number of C−C single bonds in a gas such as C_2H_2. The peak around 1.42 Å reflects the nearest distance to each carbon atom in the carbon fiber product while the peak near 2.60 Å refers to the second adjacent carbon distance of each carbon atom in the carbon fiber product. With the increase of pressure, the second peak shifts to a shorter distance due to the rise of the second nearest peak of 2.46 Å in the products of pyrolyzed PP and CTP.[13]

X-ray diffraction (XRD) spectra for CFs produced by PP and CTP at 1−6 GPa are plotted in Figure 2G and 2H. In typical graphite crystal structure and some graphitic CFs, the first peak is near $2\theta = 25°$, showing a characteristic interlayer (d_{002}) with a lattice distance of 3.44−3.45 Å in graphite, and peaks at around 45° and 80° show the atomic arrangement in (100) and (110) planes with lattice distances of 2.13 and 1.23 Å.[14,15] The XRD pattern of the initial PP precursor system and CTP precursor system before reaction exhibits three visible peaks, respectively, at $2\theta = 20°$, 45°, and 80°. Results suggest that initial PP and CTP have different interlayer structures yet a similar bonding configuration compared to graphite. As for carbonized CFs formed at 4000 K under 1−6 GPa, the second peak (45°) and third peak (80°) get lost, consistent with experimental research on pitch-based CFs.[16] With the reaction pressure increasing, the CFs formed by PP and CTP both show a more visible peak near $2\theta = 25°$, which suggests that interlayer structures similar to graphite are formed under high pressure.

On the other hand, considering the action and evolution of oxygen introduced in the stabilization process of CF's production, systems of precursors and oxygen-derived gas (CO2) are simulated as a comparison (Figures S2−S4).

Tensile Experiment. Simulation of the tensile experiment is carried out on the carbon fibers produced under different

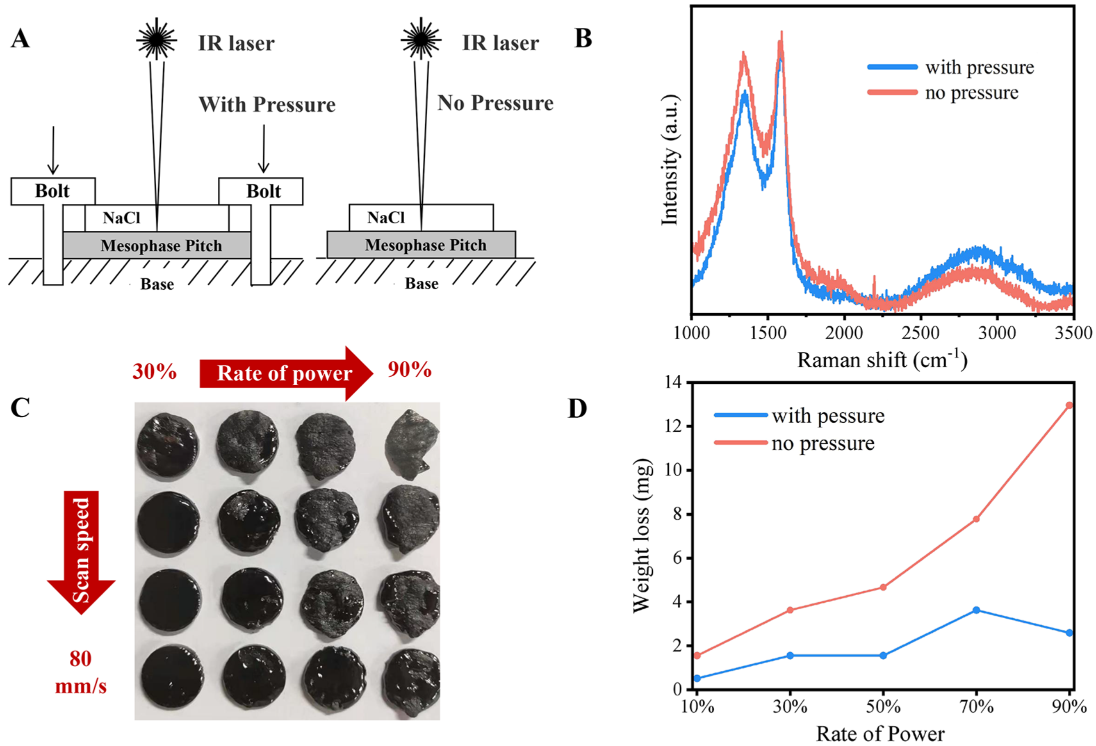

Figure 4. Experimental results. (A) Schematic of laser carbonizing process under pressurized condition and atmospheric pressure. (B) Raman spectroscopy results of laser-treated (power rate: 50%, scan speed: 40 mm/s) MP samples under pressure and without pressure. (C) Optical photos of laser-processed MP samples at different scan speeds (20−80 mm/s) and rates of power (30%−90%). (D) Weight loss of each MP sample (300 mg) after carbonization with and without pressure.

pressures as shown in Figure 3. In Figure 3A and 3B, with the increase of pressure, the tensile strengths of the PP-derived carbon fibers change from 0.2 to 2.4 GPa, with corresponding tensile moduli increase from 0.18 to 10.56 GPa. Tensile strengths of the carbon fibers derived from CTP precursor increase from 0.92 to 4.39 GPa while the tensile moduli increase from 1.4 to 22.46 GPa. Such phenomena show that the increase of reaction pressure does improve the graphitization of carbon fiber products and has a significant effect of improving their tensile strengths. To date, the current CFs on market have a range of strengths from 1.38 to 3.83 GPa), modulus 159−965 GPa, and elongation to break 0.3−0.9% of pitch-based carbon fiber.[1] The simulated tensile strengths have the same order of magnitude as the real carbon fibers, while the tensile modulus and elongation to break is 7 times smaller which can be improved by adjusting the scale of the simulation model. Compared with the mechanical properties of PP- and CTP-derived CFs under the same pressure, the CFs produced by the CTP precursors (with better thermal stability and limited decomposition pathways) are 2−5 times higher in tensile strength and modulus than those prepared by the PP precursors with higher reactivity.

Results of research aiming to investigate CFs' mechanical properties from the perspective of molecular dynamics simulation are shown in Table S1. The ranges of the tensile strength of CFs obtained by existing research are generally higher than the range of the experimental results (3−7 GPa). Joshi[14] et al. propose that the overestimation of tensile strength in their simulation test was due to the ultrahigh deformation rate and the low limit on the maximum pore size compared to the relatively small scale of unit used in the simulations. However, the tensile strength of CFs generated by our models is more likely to agree with the experimental range. The main reason for this difference is that the simulation in our study involved the whole synthesis of CFs rather than directly creating a model of CF, resulting in CF products with more complicated imperfections and thus closer to the real CFs. Since some researchers[14,17] used models assembled by few-layer structure laterally aligned and rolled up, the simulated tensile strength is closer to that of ideal monolayer graphene (130 ± 10 GPa).[18] Such results reveal a potential of high strength of fully graphitized CFs with few detects, yet these structures are difficult to synthesize from either PAN or MPs. They also compressed and heated the ladder-like structures,[14] but they did not control the simulation conditions to simulate the actual process of synthesis of CFs as in this work. Since CFs produced under different reaction conditions have great differences in mechanical properties, we suggest that the method to obtain models of CFs by simulating the reaction process is more convincing and proper.

Experimental Results. As shown in Figure 4A, a single-crystalline slice of NaCl was pressed against the MP sheet by bolt pretightening force to keep a pressurized condition through laser processing while a control group at atmospheric pressure was set. Figure 4B shows a comparison of Raman spectroscopy results of pressurized and unpressurized laser-treated MP samples (power rate: 50%, scan speed: 40 mm/s). There are three obvious peaks in the spectra of each laser-treated MP sample at shifts of about 1350, 1580, and 2700 cm^{-1}, namely, peaks D, G, and 2D peak, respectively. A decreasing trend of peak D, representing a reduction of sp^3 hybridized carbon atoms and a decrease of disordered structure in imperfect fields of graphitelike sheets,[19] and a lower I_D/I_G ratio have been both observed by changing the

https://doi.org/10.1021/acs.jpclett.2c00664
J. Phys. Chem. Lett. 2022, 13, 3283−3289

energy density of input laser (Figures S3−S4). Besides, as shown in Figure 4B, a further decreasing of peak D in Raman spectra results under the pressurized condition shows that extra pressure could help generate more ordered structures even at the same density of energy input. Peak 2D in Raman spectroscopy results of MP samples, sensitive to the stacking of layer-structure of carbon,[20] shows no obvious variation when the corresponding energy density of the laser is changed (Figures S3−S4). However, a larger range and higher height of peak 2D could be observed when the extra pressure condition was introduced, suggesting that pressurizing is effective in helping generate more multilayer-like structures or graphitic layers in MP samples (Figure S2). As shown in Figure 4C and Figures S2−S3, laser-processed MP samples at different laser scan speeds and rates of power were tested and similar trends of peak D and 2D were observed, which can be evidence of our MD simulation's conclusion about the pressure condition's effect in helping build CF's higher crystallinity. As shown in Figure 4D, the weight loss of laser-treated MP samples in pressurized carbonization, regarded as the gas generation, was less than that in unpressurized carbonization. With the rates of laser power increasing from 10% to 90% (energy density from 0.08−0.70 J/mm^2), this effect of inhibition of gas formation was increased from 57% to 83%. This effect of inhibition is similar to the MD simulation's results shown in Figure 1E and 1F, providing an explanation of how higher crystallinity is generated in the pressurized condition. A pressure cell[21] and bic-anvil type high-pressure facility[22] can be used to apply higher pressure to experiments.

In conclusion, the simulation results reveal that adding pressures (1−6 GPa) can affect the reaction activities, carbon product yields, and graphitic content evolutions during the high-temperature processes, and illustrate a significant improvement of tensile strength of both PP-derived and CTP-derived CFs. The increase of pressures rarely increases the reactant consumption rates, while high pressures suppress the degassing from the mesophase pitches and thus increase the carbon yields. The pressures promote the graphitization during heating, and the condensed CFs show exceptional mechanical properties. The CFs made of carbonized PP at 4000 K under 6 GPa provide a tensile strength as high as 2.4 GPa, while the CFs of CTP carbonized at the same condition provide a tensile strength as high as 4.39 GPa. Such results demonstrate a promising direction to manufacture ultrastrong mesophase pitch-based CFs. In the experimental work, Raman spectroscopy results show that the introduction of pressure helps build more ordered structures in MP laser processing and inhibits the gas generation by 57%−83%, which helps build higher crystallinity for as-produced fibers.

■ ASSOCIATED CONTENT

Supporting Information

The Supporting Information is available free of charge at https://pubs.acs.org/doi/10.1021/acs.jpclett.2c00664.

> Figure S1 showing schematic and calculation details of molecular dynamics simulations of MP carbonization; Table S1 showing summary of CF tensile strengths reported in molecular dynamics simulation and experimental approach; Figures S2−S4 showing details of reaction groups with oxidation process; Figures S5−S7 showing experimental results of laser-treated MP (PDF)

■ AUTHOR INFORMATION

Corresponding Authors

Xining Zang − *Department of Mechanical Engineering, Tsinghua University, Beijing 100084, China; State Key Laboratory of Tribology and Key Laboratory for Advanced Materials Processing Technology, Ministry of Education, Tsinghua University, Beijing 100084, China;* orcid.org/0000-0001-6930-8060; Email: xzang@mail.tsinghua.edu.cn

Haiyan Zhao − *Department of Mechanical Engineering, Tsinghua University, Beijing 100084, China; State Key Laboratory of Tribology and Key Laboratory for Advanced Materials Processing Technology, Ministry of Education, Tsinghua University, Beijing 100084, China;* Email: hyzhao@tsinghua.edu.cn

Authors

Yanzhuo Wei − *Department of Mechanical Engineering, Tsinghua University, Beijing 100084, China; State Key Laboratory of Tribology and Key Laboratory for Advanced Materials Processing Technology, Ministry of Education, Tsinghua University, Beijing 100084, China;* orcid.org/0000-0003-1184-9598

Jincong Chen − *Department of Mechanical Engineering, Tsinghua University, Beijing 100084, China; State Key Laboratory of Tribology and Key Laboratory for Advanced Materials Processing Technology, Ministry of Education, Tsinghua University, Beijing 100084, China*

Complete contact information is available at: https://pubs.acs.org/10.1021/acs.jpclett.2c00664

Notes

The authors declare no competing financial interest.

■ ACKNOWLEDGMENTS

X.Z. acknowledges the support by start-up funding of Tsinghua University, Tsinghua University Initiative Scientific Research Program, and the National Natural Science Foundation of China (Number 52105459). The authors thank Assist Prof. Cuiying Jian from York University in Canada for her help with codes. The authors thank Mr. Xingjian Hu from Tsinghua University in China for his help of proof reading.

■ REFERENCES

(1) Minus, M.; Kumar, S. The processing, properties, and structure of carbon fibers. *JOM* **2005**, *57* (2), 52−58.

(2) Warren, C. *Low cost carbon fiber overview*; Oak Ridge National Laboratory: Oak Ridge, TN, 2011.

(3) Yang, J.; Nakabayashi, K.; Miyawaki, J.; Yoon, S.-H. Preparation of isotropic pitch-based carbon fiber using hyper coal through co-carbonation with ethylene bottom oil. *Journal of Industrial and Engineering Chemistry* **2016**, *34*, 397−404. (a) Liu, J.; Shimanoe, H.; Nakabayashi, K.; Miyawaki, J.; Ko, S.; Jeon, Y.-P.; Yoon, S.-H. Preparation of isotropic pitch precursor for pitch-based carbon fiber through the co-carbonization of ethylene bottom oil and polyvinyl chloride. *Journal of Industrial and Engineering Chemistry* **2018**, *67*, 276−283.

(4) Li, H.; Zhu, T.; Ferralis, N.; Grossman, J. C. Charge transport in highly heterogeneous natural carbonaceous materials. *Adv. Funct. Mater.* **2019**, *29* (38), 1904283. (a) Zang, X.; Jian, C.; Ingersoll, S.; Li, H.; Adams, J.; Lu, Z.; Ferralis, N.; Grossman, J. Laser-engineered heavy hydrocarbons: Old materials with new opportunities. *Science Advances* **2020**, *6* (17), No. eaaz5231.

(5) Mochida, I.; Inaba, T.; Korai, Y.; Takeshita, K. Carbonization properties of carbonaceous substances oxidized by air blowing—II: Acid-catalyzed modification of oxidized residual oil for better anisotropic development. *Carbon* **1983**, *21* (6), 553−558.

(6) Huang, X. Fabrication and Properties of Carbon Fibers. *Materials* **2009**, *2* (4), 2369−2403.

(7) Bundy, F. Pressure-temperature phase diagram of elemental carbon. *Physica A: Statistical Mechanics and its Applications* **1989**, *156* (1), 169−178.

(8) Jian, C.; Adams, J. J.; Grossman, J. C.; Ferralis, N. Carbon fiber synthesis from pitch: Insights from ReaxFF based molecular dynamics simulations. *Carbon* **2021**, *176*, 569−579.

(9) Li, G.-Y.; Ding, J.-X.; Zhang, H.; Hou, C.-X.; Wang, F.; Li, Y.-Y.; Liang, Y.-H. ReaxFF simulations of hydrothermal treatment of lignite and its impact on chemical structures. *Fuel* **2015**, *154*, 243−251.

(10) Inagaki, M.; Park, K. C.; Endo, M. Carbonization under pressure. *New Carbon Materials* **2010**, *25* (6), 409−420.

(11) Hawthorne, H. M.; Baker, C.; Bentall, R. H.; Linger, K. R. High Strength, High Modulus Graphite Fibres from Pitch. *Nature* **1970**, *227* (5261), 946−947.

(12) Inagaki, M.; Sakai, M. Pressure Carbonization Formation of Carbon Spherules. *Tanso* **1988**, *1988* (134), 175−187.

(13) Klug, H. P.; Alexander, L. E. *X-ray diffraction procedures: for polycrystalline and amorphous materials*; 1974.

(14) Joshi, K.; Arefev, M. I.; Zhigilei, L. V. Generation and characterization of carbon fiber microstructures by atomistic simulations. *Carbon* **2019**, *152*, 396−408.

(15) Kumar, S.; Anderson, D. P.; Crasto, A. S. Carbon fibre compressive strength and its dependence on structure and morphology. *J. Mater. Sci.* **1993**, *28* (2), 423−439.

(16) Naito, K.; Tanaka, Y.; Yang, J.-M. Transverse compressive properties of polyacrylonitrile (PAN)-based and pitch-based single carbon fibers. *Carbon* **2017**, *118*, 168−183.

(17) Shi, L.; Sessim, M.; Tonks, M. R.; Phillpot, S. R. Generation and characterization of an improved carbon fiber model by molecular dynamics. *Carbon* **2021**, *173*, 232−244.

(18) Lee, C.; Wei, X.; Kysar, J. W.; Hone, J. Measurement of the elastic properties and intrinsic strength of monolayer graphene. *science* **2008**, *321* (5887), 385−388.

(19) Tuinstra, F.; Koenig, J. L. Raman Spectrum of Graphite. *J. Chem. Phys.* **1970**, *53* (3), 1126−1130.

(20) Faugeras, C.; Kossacki, P.; Basko, D. M.; Amado, M.; Sprinkle, M.; Berger, C.; de Heer, W. A.; Potemski, M. Effect of a magnetic field on the two-phonon Raman scattering in graphene. *Phys. Rev. B* **2010**, *81* (15), 155436.

(21) Hall, H. T. Some High-Pressure, High-Temperature Apparatus Design Considerations: Equipment for Use at 100 000 atm and 3000°C. *Rev. Sci. Instrum.* **1958**, *29* (4), 267−275.

(22) Zhao, J.; Yang, L.; Li, F.; Yu, R.; Jin, C. Structural evolution in the graphitization process of activated carbon by high-pressure sintering. *Carbon* **2009**, *47* (3), 744−751.

https://doi.org/10.1021/acs.jpclett.2c00664
J. Phys. Chem. Lett. 2022, 13, 3283−3289